

# Spin flips I: Evolution of the angular momentum orientation of Milky Way-mass dark matter haloes

Philip E. Bett<sup>1</sup>\* and Carlos S. Frenk<sup>2</sup>

<sup>1</sup>Argelander-Institut für Astronomie, Universität Bonn, Auf dem Hügel 71, D-53121 Bonn, Germany

<sup>2</sup>Institute for Computational Cosmology, University of Durham, South Road, Durham, DH1 3LE, UK

30 August 2018

## ABSTRACT

During the growth of a cold dark matter halo, the direction of its spin can undergo rapid changes. These could disrupt or even destroy a stellar disc forming in the halo, possibly resulting in the generation of a bulge or spheroid. We investigate the frequency of significant changes in the orientation of the angular momentum vector of dark matter haloes (“spin flips”), and their degree of correlation with mergers. We focus on haloes of mass similar to that of the Milky Way (MW) halo at redshift  $z = 0$  ( $\log_{10} M / h^{-1} M_{\odot} = 12.0 \rightarrow 12.5$ ) and consider flips in the spin of the whole halo or just its inner parts. We find that a greater fraction of major mergers are associated with large spin flips than minor mergers. However, since major mergers are rare, the vast majority (93%) of large whole-halo spin flips ( $\theta \geq 45^{\circ}$ ) coincide with *small* mass changes, not major mergers. The spin vector of the inner halo experiences much more frequent flips than the halo as a whole. Over their entire lifetimes (i.e. after a halo acquires half of its final mass), over 10% of haloes experience a flip of at least  $45^{\circ}$  in the spin of the entire halo and nearly 60 percent experience a flip this large in the inner halo. These numbers are reduced to 9 percent for the whole halo and 47 percent for the inner halo when we consider only haloes with no major mergers after formation. Our analysis suggests that spin flips (whose effects are not currently included in galaxy formation models) could be an important factor in the morphological transformation of disc galaxies.

**Key words:** cosmology: dark matter – galaxies: haloes – galaxies: evolution – methods:  $N$ -body simulations

## 1 INTRODUCTION

The acquisition and evolution of angular momentum plays a central role in the formation and evolution of cosmic structure. Early work on the acquisition of angular momentum by virialized matter clumps in a cosmological context dates back to Hoyle (1951), and the development of the linear tidal torque theory (Peebles 1969; Doroshkevich 1970a,b; White 1984; Catelan & Theuns 1996a,b; see also Porciani, Dekel & Hoffman 2002, and Schäfer 2009). This approach starts to break down as structure growth becomes non-linear (White 1984), and the subsequent evolution of dark matter halo angular momentum is usually studied using  $N$ -body simulations. This subject too has a long and rich research history, with simulations improving in size and resolution as the available computing power has increased (e.g. Peebles 1971; Efstathiou & Jones 1979; Davis et al. 1985; Barnes & Efstathiou 1987; Frenk et al. 1988; Warren et al. 1992; Cole & Lacey 1996). Recent simulations have established the distribution of the angular momentum of dark matter haloes, and its evolution, extremely accurately, from very large numbers of

well-resolved objects (e.g. Bullock et al. 2001; Avila-Reese et al. 2005; Shaw et al. 2006; Hahn et al. 2007a,b; Bett et al. 2007, 2010; Macciò et al. 2007; Macciò, Dutton & van den Bosch 2008; Knebe & Power 2008; Muñoz-Cuartas et al. 2011).

These studies have usually focused on the distribution and evolution of the angular momentum *magnitude*. In contrast, the angular momentum vector *direction* is relatively less well studied, and often only in terms of its orientation with respect to the halo shape (e.g. Warren et al. 1992; Bailin & Steinmetz 2005; Allgood et al. 2006; Shaw et al. 2006; Hayashi, Navarro & Springel 2007; Bett et al. 2007, 2010), or with other structures on different scales, such as galaxies (e.g. van den Bosch et al. 2002; van den Bosch, Abel & Hernquist 2003; Chen, Jing & Yoshikawa 2003; Gustafsson, Fairbairn & Sommer-Larsen 2006; Croft et al. 2009; Romano-Díaz et al. 2009; Bett et al. 2010; Agustsson & Brainerd 2010; Hahn, Teyssier & Carollo 2010; Deason et al. 2011), or large-scale filaments and voids (e.g. Bailin & Steinmetz 2005; Hahn et al. 2007a,b; Hahn, Teyssier & Carollo 2010; Brunino et al. 2007; Paz, Stasyszyn & Padilla 2008; Cuesta et al. 2008). Sugerma, Summers & Kamionkowski (2000) and Porciani, Dekel & Hoffman (2002) tracked the *Lagrangian*

\* Email: p.e.bett@physics.org

evolution of the mass in  $z = 0$  haloes, and showed that their spin direction changes due to non-linear evolution, with both the average deviation from the initial direction, and the scatter in that angle, increasing with time.

The motivation for studying the angular momentum of haloes is the influence it is believed to have on the formation and evolution of galaxies. In today’s cosmological paradigm, in which the dark matter is a cold collisionless particle (CDM), haloes grow hierarchically, through a series of mergers of ever larger objects. In the basic two-stage picture of galaxy formation (White & Rees 1978; White & Frenk 1991), galaxies form and evolve within these haloes, with the pattern of simple hierarchical growth modified by the more complex physical processes available to the baryons as they cycle between gas and stars. It is usually assumed that the gas and dark matter have the same initial distribution, and thus the gas in a halo initially has the same angular momentum as the halo itself. The gas then collapses to form a (rotationally supported) disc galaxy, conserving its angular momentum. Thus, the size of the galactic disc is directly related to the dark matter halo’s angular momentum (Fall & Efstathiou 1980; Mo, Mao & White 1998; Zavala, Okamoto & Frenk 2008). This basic picture is frequently implemented in so-called ‘semi-analytic’ models of galaxy formation (White & Frenk 1991), in which the modelling of the baryonic processes is grafted onto the merger histories of dark matter haloes, derived either from an  $N$ -body simulation or constructed analytically. This approach has been recently reviewed by Baugh (2006) and Benson (2010), and a comparison of different models has been carried out by De Lucia et al. (2010). It is important to emphasise that while these models incorporate the size of the dark matter angular momentum vector, they make no reference to its direction.

It has long been known that tidal forces can induce morphological changes in galaxies (Toomre & Toomre 1972). If the gravitational potential varies significantly over a short timescale, a galactic disc can be disrupted completely. Galaxy formation models thus assume that a sufficiently big galaxy merger event will destroy a disc, randomising the stellar orbits and forming a spheroid<sup>1</sup> (e.g. Toomre 1977; Barnes 1988, 1992; Barnes & Hernquist 1996; Hernquist 1992, 1993). Indeed, this has been shown to occur in merger simulations of individual objects (e.g. Naab & Burkert 2003; Bournaud, Jog & Combes 2005; Cox et al. 2006, 2008). The outcome of a merger depends on the gas richness of the participants (e.g. Stewart et al. 2008, 2009; Hopkins et al. 2009a,b, 2010), and on the details of the star formation and feedback processes triggered by the merger (e.g. Okamoto et al. 2005; Zavala, Okamoto & Frenk 2008; Scannapieco et al. 2009).

In this paper, we consider the evolution of the *direction* of the angular momentum vector (hereafter *spin* direction, for brevity) of dark matter haloes, a process that can affect the stability of a disc within the halo. Sudden, large changes in the halo spin direction are indicative of a significant disturbance to the halo. Such changes would usually accompany a halo merger<sup>2</sup>, which, in turn, could result in a galaxy merger within the halo, and potentially the destruction of an existing galactic disc (depending on the details of

the baryonic physics). However, it is also possible for tidal forces to disturb the halo *without* there being an immediate merger – for example, due to the flyby of a neighbouring halo. Recent work by Sinha & Holley-Bockelmann (2011) has shown that halo flybys indeed occur sufficiently frequently that they have a significant dynamical effect on halo systems. In such a situation, the spin direction could change significantly, even if its magnitude does not. Such ‘spin flips’ could have major consequences for the survival of a disc. The disturbance in the internal structure of the halo itself could lead to the destruction of the disc, as in a merger. However, it could also torque the disc and change its spin direction without disrupting it (Ostriker & Binney 1989), causing it instead to become misaligned relative to the direction of new infalling material. In due course, the accretion of misaligned material could lead to the disruption of the disc and the formation of a spheroid. Such spin flips provide a mechanism of spheroid formation that is not currently considered in galaxy formation models.

$N$ -body and hydrodynamical simulations have shown that large, rapid changes to dark matter halo spin directions do indeed occur. Okamoto et al. (2005) remarked that their simulated galaxy, which had formed a small disc, flipped its orientation. It then began to accrete gas in a direction nearly perpendicular to the original disc which was subsequently transformed into a bulge with a new disc later forming<sup>3</sup>. Romano-Díaz et al. (2009) analysed haloes in simulations both with and without baryons, at very high time resolution. They found that, although the spin magnitude changes by a factor of  $\sim 2$ – $3$  after a major merger, the orientation can change much more drastically, by  $\gtrsim 180^\circ$ . Furthermore, such large changes in angular momentum orientation are not restricted to major mergers. In the simulations with baryons, the authors also found that the DM halo, stellar disc, and gas component can often flip orientation with respect to each other as the system evolves, even at late times where there are few major mergers. Scannapieco et al. (2009) found that misalignment of a stellar disc with the accreting cold gas can sometimes cause mass to transfer from the disc to a spheroidal component, sometimes destroying the disc (and sometimes allowing a new disc to be formed later).

In this and subsequent papers, we use a dark matter  $N$ -body simulation to assess the frequency of spin flip events occurring in the lifetime of haloes. We do not model baryonic physics, and instead concentrate on quantifying the amplitude and frequency of spin flips. Our aim in this first paper is to make an initial assessment of the importance of spin flips as a potential mechanism for the disruption of discs and the formation of spheroids. We focus here on those haloes whose mass at  $z = 0$  is similar to that of the Milky Way (MW). We perform a more in-depth study on the distribution of spin flips in a subsequent paper (Bett & Frenk 2011, hereafter Paper II).

The outline of this paper is as follows. In section 2, we describe the  $N$ -body simulation we use and our analysis procedure, including details of halo identification, merger trees, halo selection, and the definition of the quantities of interest here: the fractional mass change, and the spin orientation change. We present our results in section 3, describing both the joint and cumulative distributions of spin flip and merger events, and investigate the frequency of spin flips over the course of halo lifetimes. We discuss our conclusions in section 4.

<sup>1</sup> Such a spheroid is often distinguished from a so-called pseudobulge (e.g. Kormendy & Kennicutt 2004; Freeman 2008). Pseudobulges are thought to form through secular evolution of the disc.

<sup>2</sup> In the case of a major merger, the resulting spin direction is correlated with the net orbital spin of the progenitors (Faltenbacher et al. 2005). Furthermore, there is a degree of correlation in the infall directions of satellite haloes (e.g. falling along filaments, Knebe et al. 2004; Libeskind et al. 2005; Lovell et al. 2011; Libeskind et al. 2011).

<sup>3</sup> A preliminary analysis of this system, in the spirit of the present paper, can be seen in Bett (2010).

$L_{\text{box}}$ $h^{-1}\text{Mpc}$	$N_{\text{part}}$	$m_{\text{p}}$ $10^7 h^{-1}\text{M}_{\odot}$	$\eta$ $h^{-1}\text{kpc}$
100	$729 \times 10^6$	9.518	2.4

**Table 1.** Simulation parameters for the hMS simulation: box size, numbers and masses of particles, and gravitational softening  $\eta$ .

$\Omega_{\Lambda 0}$	$\Omega_{\text{M}0}$	$\Omega_{\text{b}0}$	$h$	$n$	$\sigma_8$
0.75	0.25	0.045	0.73	1.0	0.9

**Table 2.** Cosmological parameters (at  $z = 0$ ) for the hMS simulation used in this paper: cosmological density parameters  $\Omega_{i0}$ , the Hubble parameter  $h$ , the spectral index  $n$ , and  $\sigma_8$  is the linear theory mass variance in spheres of radius  $8h^{-1}\text{Mpc}$  at  $z = 0$ . As with the Millennium Simulation, these parameters were chosen to be good matches to the results of the 2dF galaxy redshift survey (Colless et al. 2001; Percival et al. 2002) and the first year results of the WMAP microwave background satellite (Spergel et al. 2003).

## 2 SIMULATION DATA AND ANALYSIS

In this section we describe the  $N$ -body dark matter simulation we use and the associated halo catalogues and merger trees constructed to link each halo with its descendent in a subsequent output time. We calculate various halo properties, and use the merger trees to describe how these properties evolve over the lifetime of each halo.

### 2.1 The hMS simulation, haloes and merger trees

We use the hMS cosmological dark matter simulation. This was carried out using the same L-GADGET-2 code and  $\Lambda\text{CDM}$  cosmological parameters as the Millennium Simulation (Springel et al. 2005), but with a smaller box size and higher resolution<sup>4</sup>. Relevant simulation parameters are shown in Table 1, while the assumed cosmological parameters are shown in Table 2. Throughout, we refer to cosmological density parameters  $\Omega_i(z) = \rho_i(z)/\rho_c(z)$ , in terms of the mass density<sup>5</sup> of component  $i$  and the critical density  $\rho_c(z) = 3H^2(z)/(8\pi G)$ , where  $H(z)$  is the Hubble parameter. We use a subscript zero to denote parameters evaluated at  $z = 0$ , and parameterise the present day value of the Hubble parameter as  $H_0 = 100h \text{ km s}^{-1} \text{ Mpc}^{-1}$ .

As with the Millennium Simulation, at each simulation snapshot particle groups were identified on-the-fly according to the friends-of-friends algorithm (FoF), with a linking length parameter of  $b = 0.2$  (Davis et al. 1985). Subsequently, self-bound substructures within these groups were found using the SUBFIND algorithm (Springel et al. 2001). Finally, the progenitors and descendants of each particle group were found, creating a ‘merger tree’ structure allowing haloes to be tracked over time. The merger tree algorithm (and associated halo definition) used is that described in Harker et al. (2006), which was originally designed for use with the GALFORM semi-analytic galaxy formation model and the Millennium Simulation<sup>6</sup> (Helly et al. 2003; Bower et al. 2006). Since

the construction of haloes and mergers trees from particle groups in discrete snapshots is essential for the current work, we will now describe this process in more detail.

The preliminary set of haloes consists, at each snapshot, of the FoF particle groups, which in turn contain the self-bound substructures identified by SUBFIND (these include the main body of the halo, plus less massive subhaloes), as well as so-called ‘fuzz’ particles not gravitationally bound to any structure in the halo. It is well known that the purely spatial nature of the FoF algorithm allows multiple objects to be linked together spuriously, in the sense that although they are close together they might not necessarily be physically connected. A common example is that of two close objects linked with a tenuous bridge of particles, which the FoF algorithms identifies as a single ‘halo’ (see Bett et al. 2007 for a detailed discussion and comparison of the effect of groupfinders on the measured halo angular momentum and related properties).

Including additional physical information – e.g. gravitational binding from SUBFIND, and temporal evolution from merger trees – allows the operational definition of a halo to be refined, to match better our physical intuition of what a halo is, and thus, when used in conjunction with semi-analytic models of galaxy formation, to allow better comparisons with both observations and hydrodynamic simulations. Following Wechsler et al. (2002), a ‘splitting’ algorithm is applied to the basic FoF halo catalogues, whereby spuriously linked subhaloes are split off from their original FoF groups and identified as separate haloes in their own right. A subhalo is split off from its original FoF parent if it satisfies at least one of the following conditions: (1) The distance between the subhalo centre and the parent centre is more than twice the half-mass radius of the parent; or (2) the subhalo still has more than 75% of the mass it had when it was last identified as a separate halo. This yields halo catalogues containing more objects than the corresponding FoF catalogues. Bett et al. (2007) showed that these ‘merger tree haloes’ are a great improvement on both the simple FoF groups and groups found from a simple spherical overdensity criterion.

Merger trees for these haloes are constructed by tracking the particles that constitute the subhaloes between each snapshot, starting at early times and continuing to redshift  $z = 0$ . Each halo or subhalo can have at most one descendent in a later snapshot. The most bound 10% of a subhalo’s mass (or 10 most bound particles if that is more massive) is located in the next snapshot. Occasionally, these particles might no longer reside in a subhalo in the next snapshot: the subhalo might have temporarily dropped below SUBFIND’s detection limit, or might be passing through a high density region and be interpreted as unbound matter around that density peak. In practice therefore, the next five snapshots are scanned to find the earliest time when these particles are again in subhaloes. The descendent subhalo is then identified as the subhalo containing the largest number of those most bound particles. The descendent of a halo is identified as the halo whose most massive substructure (i.e. the main self-bound halo component) is the descendent of its own most massive substructure.

It is possible that a subhalo’s mass ends up distributed between two (or more) subhaloes in a subsequent snapshot. While one will be identified as the descendent, the other will be left as a separate ‘orphan’ object without a progenitor. This situation is known as a de-merger, and is a physical effect separate to the splitting of groups described above – here, sets of particles physically end up in separate objects as the simulation evolves.

The end result of this process is a catalogue of haloes (groups of self-bound substructures) identified at each snapshot, with at most one descendent and one or more progenitors. Each halo iden-

<sup>4</sup> The hMS simulation was previously used by Neto et al. (2007), Gao et al. (2008), Boylan-Kolchin et al. (2009), Libeskind et al. (2009), and Bett et al. (2010).

<sup>5</sup> The equivalent mass density of the cosmological constant,  $\Lambda$ , is  $\rho_{\Lambda} = \Lambda c^2/(8\pi G)$ .

<sup>6</sup> In particular, they correspond to the DHaLo tables in the Millennium Simulation database (Lemson & the Virgo Consortium 2006)

tified at  $z = 0$  is the root of its own tree, which branches into many progenitor haloes at preceding output times. In this paper, we study the evolution of properties of individual haloes that at  $z = 0$  have a mass corresponding roughly to that of the Milky Way. After identifying an appropriate halo at  $z = 0$ , we track its evolution back by finding its most massive progenitor at the preceding snapshot, then finding the most massive of *that* halo’s progenitors, and so on.

It is important to note that, just like the halo definition and galaxy formation model, the halo merger tree algorithm is not by any means unique – even within a given  $N$ -body simulation. The halo merger trees used for the “MPA” semi-analytic models of the Millennium Simulation (e.g. Springel et al. 2005 and De Lucia & Blaizot 2007) in fact track the binding-energy-weighted mass in the SUBFIND subhaloes. Other methods that use splitting/stitching algorithms similar to the one used here include those by e.g. Fakhouri & Ma (2008, 2009), Genel et al. (2009); see also Maller et al. (2006). Tweed et al. (2009) provide a recent detailed study of halo definition and merger tree algorithms.

## 2.2 Halo property catalogues

Various properties of the haloes are computed at each output time. Properties are computed in the centre-of-momentum frame of each halo, and in physical rather than comoving coordinates. Each halo consists of a set of  $N_p$  particles, with each particle  $i$  having mass  $m_i = m_p$ , position  $\mathbf{x}_i$  and velocity  $\mathbf{v}_i$ . The halo mass is therefore  $M_h = \sum_{i=1}^{N_p} m_i = N_p m_p$ . The halo centre is taken to be the location of the gravitational potential minimum of its most massive substructure, as found by SUBFIND. We define an approximate “virial” radius,  $R_{\text{vir}}$ , for the halo<sup>7</sup> by growing a sphere from the halo centre and computing the density of the halo particles within. We locate  $R_{\text{vir}}$  at the radius at which the density enclosed drops below a certain threshold value computed at that snapshot,  $\rho_h = \Delta_c(z)\rho_c(z)$ . The threshold overdensity with respect to critical,  $\Delta_c(z)$ , is determined from the spherical collapse model (Eke, Cole & Frenk 1996), using the fitting formula of Bryan & Norman (1998):

$$\Delta_c(z) = 18\pi^2 + 82(\Omega_M(z) - 1) - 39(\Omega_M(z) - 1)^2 \quad (1)$$

In the case of the flat  $\Lambda$ CDM universe used here,  $\Omega_M(z) = \Omega_{M0}a^{-3}/\chi(z)$  and  $\rho_c(z) = \rho_{c0}\chi(z)$ , where the expansion factor  $a = (1+z)^{-1}$  and we define  $\chi(z) = \Omega_{M0}a^{-3} + \Omega_{\Lambda0}$  for convenience.

We compute halo energies as in Bett et al. (2007, 2010). The kinetic energy of a halo is given by  $T = \frac{1}{2} \sum_{i=1}^{N_p} m_i v_i^2$ , and the potential energy is computed as a double sum over a random sample of 1000 particles, using the same smoothing kernel for gravitational softening as in the simulation itself. We only use the energies for some broad selection criteria (described below), and random sampling provides a good approximation.

In this paper, we are mostly interested in the halo angular momentum vector,  $\mathbf{J} = \sum_{i=1}^{N_p} m_i \mathbf{x}_i \times \mathbf{v}_i$ . We also define an inner halo angular momentum,  $\mathbf{J}_{\text{inner}}$ , using the particles within  $r_{\text{inner}} = 0.25R_{\text{vir}}$ .<sup>8</sup>

## 2.3 Halo selection

We need to select haloes at each snapshot from which reliable measurements of angular momentum can be made. The halo has to

be well defined, that is, both well resolved (consisting of a sufficiently large number of particles), and reasonably relaxed (close to being virialised). Furthermore, the angular momentum magnitude cannot be too small: if the angular momentum vectors of most particles are in opposite directions and cancel, then the net direction will be dominated by very few particles and will not be robust. We follow the approach of Bett et al. (2010), defining a scaled angular momentum<sup>9</sup>  $\tilde{j}$  as the ratio of the specific angular momentum  $j$  to that of a single particle in a Keplerian orbit,  $\tilde{j} = j / \sqrt{GM_h R_{\text{vir}}}$ , along with the analogous quantity for the inner halo  $\tilde{j}_{\text{inner}} = j_{\text{inner}} / \sqrt{GM_{\text{inner}} 0.25R_{\text{vir}}}$ . As a basic way of assessing virialisation, we compute  $Q = 2T/U + 1$ , which should be around zero for a virialised halo. We use the same critical values for selection as Bett et al. (2010); in particular, haloes that pass the following three criteria are retained:

$$N_p \geq 1000 \quad (2)$$

$$|Q| \leq 0.5 \quad (3)$$

$$\log_{10} \tilde{j} \geq -1.5 \quad (4)$$

(When considering changes to the inner halo, the criteria for  $N_p$  and  $\tilde{j}$  are replaced by equivalent ones for  $N_{p,\text{inner}}$  and  $\tilde{j}_{\text{inner}}$ .) Note that these selection criteria are applied to haloes *separately at each given snapshot*, rather than once for their whole lifetime. Haloes can be excluded at one timestep (including at  $z = 0$ ), but still retained for study at subsequent or preceding timesteps.

In addition to the particle number cut above, we restrict our analysis to haloes that at  $z = 0$  have masses similar to that of the Milky Way halo. That is, we retain only haloes whose final mass is  $10\,506m_p \leq M_0 < 33\,224m_p$ , equivalent to the mass range  $12.0 \leq \log_{10}(M_0/h^{-1}M_\odot) < 12.5$  (see Table 1).

A visual inspection of the coevolution of different halo properties for individual haloes suggested that a further two selection criteria should also be applied. Firstly, the early life of a halo is very chaotic, with a high rate of mass accretion, mergers, and general instability in halo properties. So that our results are not dominated by this early period, before the halo has properly formed (in some sense), we restrict our analysis to the time period after the final time when  $M(z) < 0.5M_0$  (where  $M_0$  is the halo mass at  $z = 0$ ). This corresponds to a commonly used simple definition of halo “formation” time (e.g. Lacey & Cole 1993; Sheth & Tormen 2004; Hahn et al. 2007a; Neto et al. 2007; Giocoli et al. 2007; Li, Mo & Gao 2008, and references therein). Since stellar disks are unlikely to survive the early chaotic phase of halo formation (Parry, Eke & Frenk 2009), restricting attention to the period after the halo has formed is appropriate for investigating the frequency of spin flips that could alter the morphology of a disk galaxy. This condition must be borne in mind when interpreting the statistics that we present below. We plot the formation times of these haloes, according to this definition, in Fig. 1. The peak in the distribution is around haloes forming at  $z \approx 1$ .

Secondly, we found that there are some occasions in which the halo finder or merger tree algorithms make unphysical choices for which subhaloes to incorporate into which haloes. For example, if a satellite halo was orbiting near the edge of a halo, then it might “merge” at one snapshot, then be identified as a separate object again later, only to finally merge again afterwards. During such events, the angular momentum vector might appear to swing around wildly, as a large mass at large radius would be added to,

<sup>7</sup> Note that we do not use  $R_{\text{vir}}$  as a boundary for our halo. However, it provides a useful scale for the physical halo size needed in other properties.

<sup>8</sup> This is similar to Bett et al. (2010), although there we defined  $r_{\text{inner}} = 10^{-0.6}R_{\text{vir}} \approx 0.25R_{\text{vir}}$

<sup>9</sup> Note that  $\tilde{j}$  is identical to the alternative spin parameter  $\lambda'$  introduced by Bullock et al. (2001), modulo a factor of  $\sqrt{2}$ .

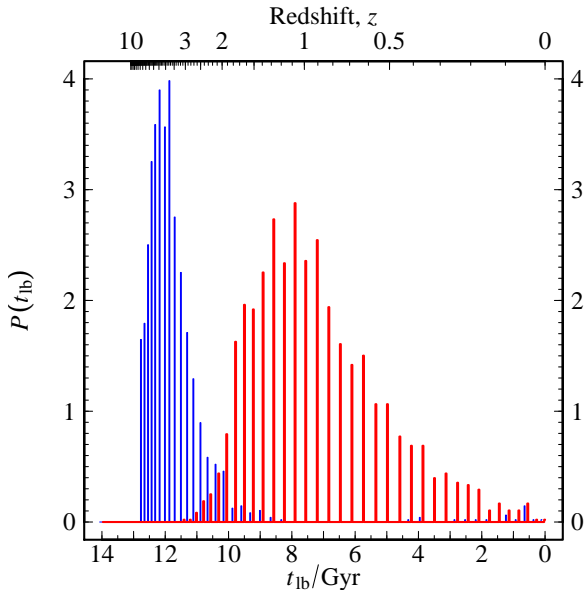


**Figure 1.** Histogram of formation times (red) and initial detection (‘start’) times (blue) for haloes that have MW masses and pass our standard selection criteria at  $z = 0$ , in terms of lookback time,  $t_{\text{lb}}$ , and redshift. The formation and start times are computed using haloes at  $z > 0$  that pass just the  $N_p$  selection criterion. There is a histogram spike at each snapshot from  $z < 6.2$ ; the blue spikes are offset slightly to make them visible.

then removed from, the total halo  $\mathbf{J}$ . Since such changes are *not* due to a physical change in the halo angular momentum, but instead are due to uncertainty in where to draw the halo boundary, we should exclude such events. It turns out that such events also cause large changes in the halo kinetic energy  $T$ , as the bulk velocity of the satellite halo will be incorporated into the main halo greatly increasing its net velocity dispersion. Thus, such events can be identified by considering the arithmetic change in the virialisation parameter  $Q$ ; since the potential energy  $U < 0$  and does not change much, an apparent sudden increase in  $T$  makes  $Q$  appear to decrease suddenly. By examining various cases, we chose to exclude events<sup>10</sup> that have  $\Delta Q \leq -0.3$ .

Finally, we note that we analyse the halo population over the redshift range  $z < 6.2$ ; in any case, the effects we describe will be most visible at low redshift. As shown in Fig. 1, there are 46 snapshots over this redshift range, with 23 over the period  $z < 1$ .

## 2.4 Evolution of halo properties

Combining the merger tree data with the halo property catalogues at each snapshot, we can obtain the evolution of each halo property, for each halo identified at  $z = 0$ . We are most interested in the relationship between the *change* in halo mass and the *change* in halo spin orientation, from snapshot to snapshot. That is, we focus on two *differential* halo properties, the fractional mass change

$$\Delta\mu(t) := \frac{M(t) - M(t - \tau)}{M(t)}, \quad (5)$$

and the angular change in spin orientation

<sup>10</sup> Since this effect is due to uncertainties in the halo boundary, we do not apply this exclusion criterion when considering the inner halo spin.

$$\cos \theta(t) := \frac{\mathbf{J}(t) \cdot \mathbf{J}(t - \tau)}{|\mathbf{J}(t)| |\mathbf{J}(t - \tau)|}, \quad (6)$$

where  $t$  is the time at which the quantity is measured, and  $\tau$  is the timescale over which we measure the halo property change; the time  $t - \tau$  precedes the time  $t$ .

In principle, we could simply look at the difference in halo properties at adjacent snapshot times. However, since the snapshots in the hMS are not evenly spaced in time, this would not be a fair way to analyse events in haloes at different times (the intersnapshot time varies between  $\sim 0.1$ – $0.4$  Gyr for  $z \lesssim 6$ ). Instead, we choose a constant value for  $\tau$ , and simply linearly interpolate the halo property in question between the values at the snapshots before and after the time  $t - \tau$ . The simulation snapshots are in fact sufficiently closely spaced in time that this interpolation is accurate.

We will refer to the property (or property change) of a given halo at a given snapshot as an *event*. We shall use some fiducial critical values to divide the distribution of events to aid interpretation. We shall consider a spin direction change of at least  $\theta_0 = 45^\circ$  to be ‘large’, and a fractional mass change of more than  $\Delta\mu_0 = 0.3$  to correspond to a major merger<sup>11</sup>. For the sake of brevity, we shall refer to events with  $\Delta\mu \leq 0.3$  as minor mergers, even though they could be smooth accretion (i.e. not the merging with a satellite halo), or even mass loss.

The choice of event timescale is non-trivial, since any characteristic halo dynamic timescale is likely to depend on halo mass and size (and therefore also on cosmology and time) – but we wish to use a single timescale for all haloes at all times, so that we can compare events at different times in different haloes fairly. The timescale we choose will therefore be only an approximation for the actual timescale of any particular halo.

We consider the orbital timescale for a particle in a Keplerian orbit at the half-mass radius  $R_{1/2}$  of a model halo bounded by the radius enclosing the density  $\Delta_c(z)\rho_c(z)$ . For a halo of a given mass, a concentration can be found by assuming an NFW density profile (Navarro, Frenk & White 1996, 1997) and using the redshift dependent mass-concentration relation of Muñoz-Cuartas et al. (2011). The half-mass radius for a halo of a given concentration can then be found using the fitting formula of Łokas & Mamon (2001), allowing a timescale to be computed as

$$\tau_{1/2} = \sqrt{\frac{2R_{1/2}^3}{GM}}. \quad (7)$$

For haloes in the mass range we consider in this paper,  $\tau_{1/2}$  varies from about 0.37 Gyr at  $z = 1$  to about 0.63 Gyr at  $z = 0$ . (The values computed analytically using the fitting formulae outlined above agree with those measured directly from haloes in the simulation.) We therefore take a fixed value for the event timescale of  $\tau = 0.5$  Gyr, although we note that we do not expect our results to depend qualitatively on the *exact* value used; for some key results we show their dependence on  $\tau$ . We will consider the choice of  $\tau$  in more detail in Paper II. It is important to note that  $\tau$  is the timescale for our measurements of halo changes, and the physical timescale of flips or mergers can be much shorter.

<sup>11</sup>  $\Delta\mu$  is only restricted to be  $< 1$ ; a value of  $\Delta\mu = \frac{1}{3}$  means that the mass has increased by 50%. If  $\Delta\mu \geq \frac{1}{2}$ , then the halo has more than doubled in mass; we expect this to be rare, since we are, by definition, comparing with the most massive progenitor. Negative values of  $\Delta\mu$  are possible, corresponding to mass *loss* between snapshots;  $\Delta\mu = -1$  means that the halo has lost 50% of its previous mass.

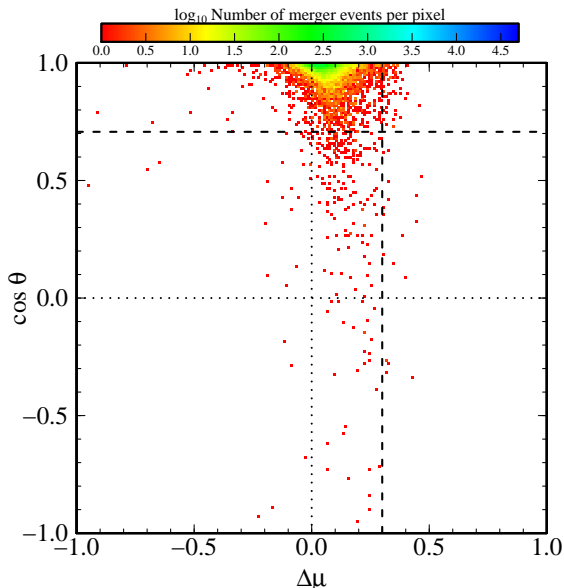


**Figure 2.** Distribution of events as a function of fractional mass change,  $\Delta\mu$ , and spin orientation change,  $\cos\theta$ . Dotted lines mark the origin and dashed lines indicate our fiducial critical values for major mergers ( $\Delta\mu \geq 0.3$ ) and large flips ( $\theta > 45^\circ$ ).

Using the whole-halo selection criteria described in section 2.3 gives us a population of 35 279 events. When we select instead for the inner halo spin, we have 29 889 events.

### 3 RESULTS

#### 3.1 The distribution of flips and mergers

We start by examining how changes in the spin orientation of the halo correlate with changes in the halo mass that occur at the same time.

##### 3.1.1 Distribution of whole halo flip and merger events

The distribution of events for MW-final-mass haloes is shown in Fig. 2. There are very few major mergers or large flips, with most events located around “no change” ( $\cos\theta \approx 1$ ,  $\Delta\mu \approx 0$ ). Most of the spread in  $\cos\theta$  is located between no mass change and our fiducial threshold for major mergers ( $\Delta\mu = 0.3$ ).

Since we are interested in mergers and flips above and below some critical value, rather than *at* some value, it is useful to examine the cumulative distribution functions (CDFs) of the data. The CDF of  $\cos\theta$  is shown in Fig. 3. We can see that, if we consider just events without major mergers ( $\Delta\mu \leq 0.3$ ), then only a very small fraction have large flips: about 0.7% have flips of  $45^\circ$  or more. If we select only major mergers, then since we have now excluded the main peak of the distribution we find a much higher proportion of events with large flips: about 17% have flips of at least  $45^\circ$  (although the major mergers themselves represent only 0.3% of the total event distribution).

We can also consider the CDF of  $\Delta\mu$  (Fig. 4). In this case, if we select just large flips, we find that the vast majority (93% of those with  $\theta \geq 45^\circ$ ) coincide with minor mergers ( $\Delta\mu \leq 0.3$ ).

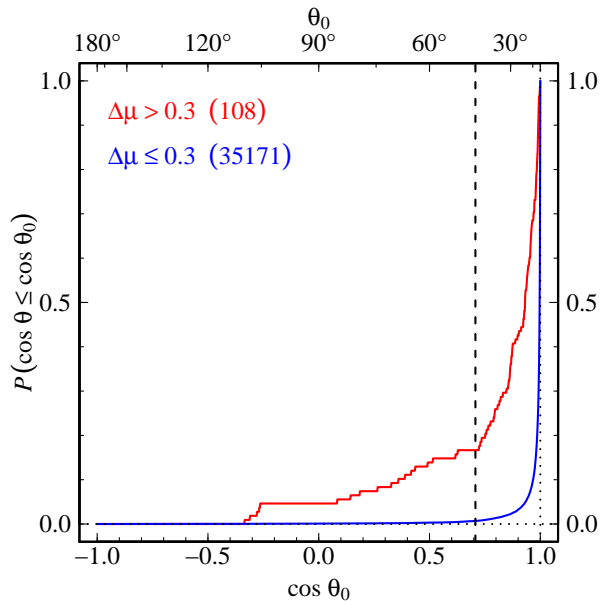


**Figure 3.** Cumulative distribution of events with spin misalignments of at least  $\theta_0$  degrees. The dashed line shows our fiducial value of  $\theta_0 = 45^\circ$ . We show results for a limiting merger fraction of  $\Delta\mu_0 = 0.3$  (red: major mergers; blue: minor mergers). The number of events in each case is written in the legend.

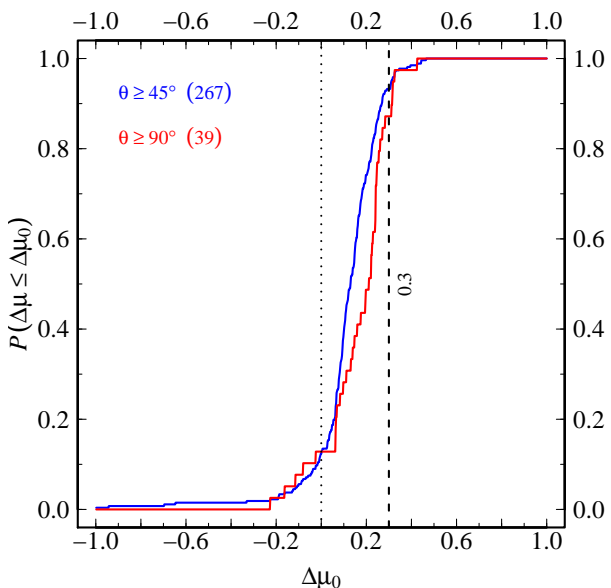


**Figure 4.** Cumulative distribution of events with fractional mass change of  $\Delta\mu_0$  or less, for events with large spin flips (red: at least  $45^\circ$ ; blue: at least  $90^\circ$ ). The dashed line shows our fiducial value of  $\Delta\mu_0 = 0.3$ , and the dotted line marks no mass change.

##### 3.1.2 Distribution of flips of the inner spin

The distribution of flips of the inner halo angular momentum is more directly relevant when considering the stability of galaxies that might form within. The joint distribution of events as a function of the inner halo spin direction change and the mass change of the whole halo is shown in Fig. 5. In comparison to the distribution for

total halo spin flips, the inner halo exhibits a far greater spread to low-cos  $\theta$ .

Cumulative distributions are shown in the middle and right panels of Fig. 5. We find that the frequency of minor merger events (the blue line in the middle panel) that have a large inner spin flip is about 6.7%, which is a significant increase on that for total halo flips shown in Fig. 3 (0.7%). The fraction of major merger events that also have significant inner flips is slightly increased, to 26.6%. Selecting just large flips (right panel), the frequencies are similarly increased compared to the total halo flip distribution: 98.9% of flips of at least  $45^\circ$  coincide with minor mergers, dropping slightly to 97.3% for flips of at least  $90^\circ$ .

### 3.2 Spin flips over halo lifetimes

While it is important to understand the overall frequency of flip events, and their tendency to correlate with mergers, we are also concerned with the frequency of spin orientation changes over the course of halo lifetimes.

#### 3.2.1 Flips and coincident mergers as a function of flip duration

An important question to answer is what is the likelihood of a halo exhibiting a spin flip (of a given magnitude  $\theta_0$  and measured over a timescale  $\tau$ ) at some point during its lifetime? This can be further specified by restricting attention to spin flips that do (or do not) coincide with a major merger.

We answer these questions in Fig. 6, for a range of values of  $\theta_0$  and  $\tau$ , given our fiducial major merger threshold of  $\Delta\mu_0 = 0.3$ . As one would expect, the likelihood of getting a spin flip increases as one considers longer timescales or flips of smaller magnitudes. (The steps are an artefact of the discrete and irregular snapshot times, coupled with our interpolation scheme and relatively small halo population. Increasing  $\tau$  causes jumps as the snapshots used for interpolation change, and this occurs at different values of  $\tau$  for haloes in different snapshots. With a larger halo sample, the lines become smooth curves, which we demonstrate in Paper II.)

Quantitatively, considering flips using our fiducial values of  $\theta_0 = 45^\circ$  and  $\tau = 0.5$  Gyr, we find that 10.5% of Milky-Way final mass haloes (172 haloes) experience such a flip at some point in their lives. If we consider just those for which such flips coincide with major mergers, this drops to just 0.9% (14 haloes). We find that 10.1% of haloes (166) experience a large flip without a major merger.

We can construct a similar plot for changes to the inner halo angular momentum direction, which we show in Fig. 7. There is an increased tendency for haloes to have flips that do not coincide with major mergers, for all flip angles  $\theta_0$  and timescales  $\tau$ . For example, for our fiducial choice of  $\tau$  and  $\theta_0$ , we find that 58.5% (783 haloes) have large flips at some point in their lifetimes; a similar number have such flips without a major merger (58.4%, 782 haloes). For those that have a major merger at the same time as such a flip, the fraction is still very low, at 1.1% (15 haloes).

#### 3.2.2 Flips in haloes without mergers

Finally, we consider the particular case of haloes which have quiet merger histories, i.e. which do not have a major merger after their formation epoch (i.e. after  $z \approx 1$ ; see Fig. 1). This case is interesting because it includes those haloes most likely to host a disc.

The results are shown in Fig. 8 (left panel). We find that 9.0%

of haloes without major mergers since formation nevertheless have a flip of their total spin of at least  $45^\circ$  (185 haloes out of 2046). Since there are very few major mergers after formation even for our total halo population (as shown in Fig. 2), this figure does not change much if we do *not* apply the no-major-merger restriction: 9.8% of such haloes have large flips, corresponding to 210 haloes out of 2146. On the other hand, 25% of the 100 haloes *with* major mergers since formation have spin flips of at least  $45^\circ$ .

If we consider flips to the inner halo spin vector (right panel of Fig. 8), then as we have seen before, there is an increased likelihood for a halo to experience a significant flip. For haloes without major mergers after formation, 47% have large flips of their inner spin (946 out of 2006). Since large spin flips, particularly of the inner halo, are so common during the lifetimes of Milky Way-mass haloes, it seems unlikely that all such flips will result in the eventual destruction of a disc, although some form of dynamical disturbance is to be expected. The effect of the flips on the structure of the disc cannot, of course, be determined with our dark matter only simulations.

## 4 DISCUSSION AND CONCLUSIONS

We have investigated the idea that spin flips – large and rapid changes in the orientation of the angular momentum of dark matter haloes – can occur without a major halo merger. These flips are a manifestation of strong tidal interactions and can be caused by minor mergers or by flybys of a neighbouring object. Spin flips could, in principle, cause enough of a dynamical disturbance in the halo to disrupt or even destroy a galactic disc, perhaps resulting in the formation of a bulge or spheroid. Evidence for such dramatic outcomes have been seen in simulations of the formation of individual galaxies (e.g. Okamoto et al. 2005; Scannapieco et al. 2009). However, semi-analytic galaxy formation models do not take into account the potentially destructive effects of spin flips. The only processes that can transform discs into spheroids in current models are major mergers and disc instabilities caused by the accretion of matter onto the disc.

Our goal in this paper has been to determine the frequency of spin flips during the lifetime of a galactic halo. We have distinguished between flips affecting the entire halo and flips affecting only the inner parts of the halo which, at face value, would seem the most relevant for the stability of the disc. We have, for this initial exploration, chosen to focus on haloes that are roughly the mass of the Milky Way’s halo at  $z = 0$ , i.e. between  $10^{12}$  and  $10^{12.5} h^{-1} M_\odot$  and that are reasonably relaxed, as would be expected for haloes in which discs can form. In Paper II we will extend this analysis to haloes of a much larger range in mass.

We have found that, while the majority of what we have termed “events” (i.e. changes to a halo between a given snapshot  $t_i$  and a preceding time  $t_i - \tau$ ) cause only small variations in both mass and spin direction, the distribution has a significant scatter and a large tail of significant variations in spin direction. The vast majority of large spin flips affecting the whole halo occur without an accompanying major merger (93 per cent of events with angular change in spin direction  $\theta > 45^\circ$  have a fractional mass change  $\Delta\mu \leq 0.3$ ). However, such large halo-wide spin flips are a rare occurrence: only 0.7 per cent of non-major-merger events ( $\Delta\mu \leq 0.3$ ) have  $\theta > 45^\circ$ .

Over the course of their lifetime (i.e. over the period after the halo has acquired half of its final mass), we find that 10.5 per cent of MW final-mass haloes experience at least one spin flip of  $\theta > 45^\circ$

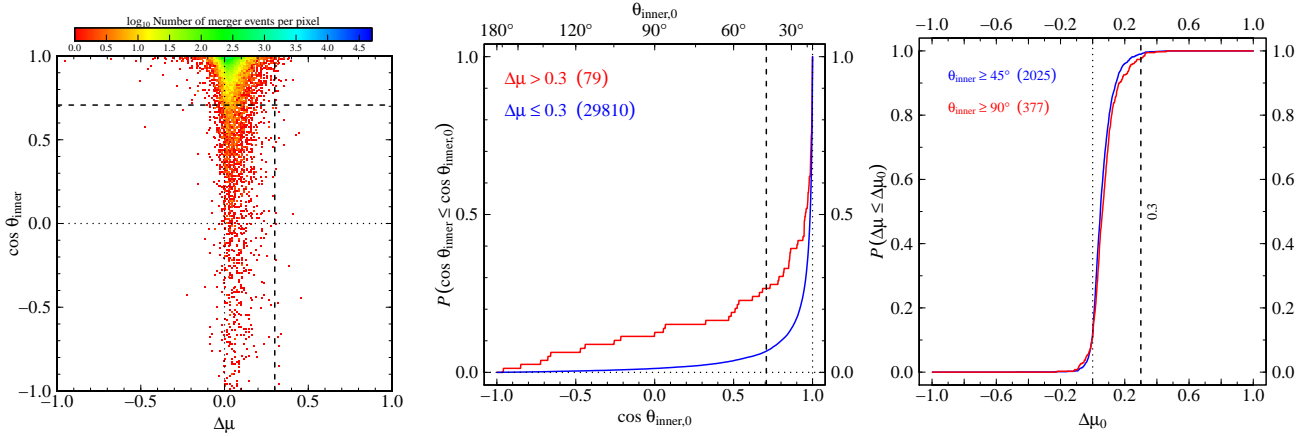


**Figure 5.** Left: event distribution as a function of the inner halo spin flip versus the total halo fractional mass change. Middle: Cumulative distribution function for merger events with inner spin misalignments of at least  $\theta_{\text{inner},0}$  degrees, for major merger events (red) and minor mergers (blue). Right: Cumulative distribution of events with mass changes  $\leq \Delta\mu_0$ , for spin flips of at least  $45^\circ$  (blue) and at least  $90^\circ$  (red).

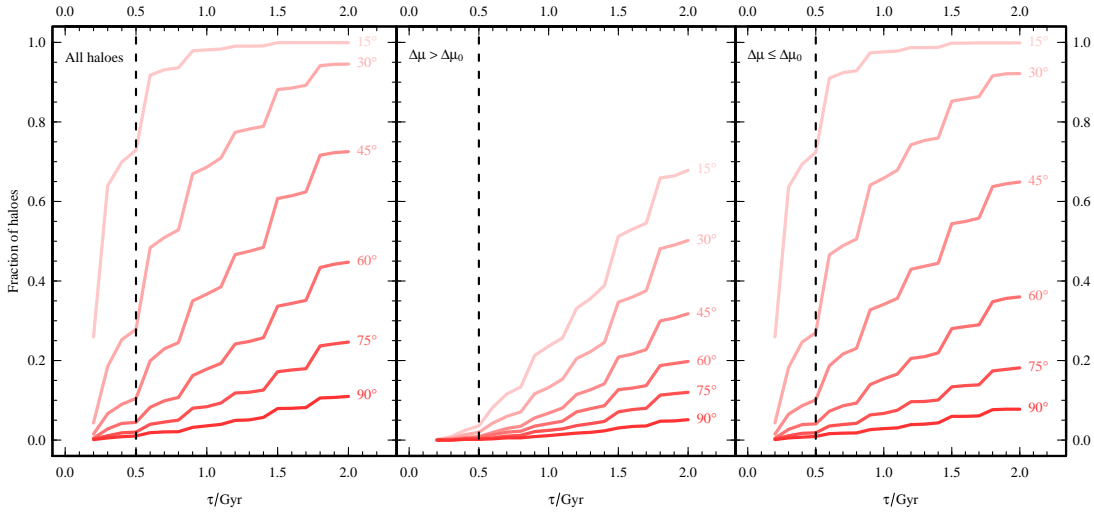


**Figure 6.** The fraction of haloes with Milky-Way masses at  $z = 0$  that have at least one flip of at least  $\theta_0$  and duration  $\tau$  (left). Middle: same, but adding the constraint that the flip must coincide with a major merger  $\Delta\mu > \Delta\mu_0$ , with  $\Delta\mu_0 = 0.3$ . Right: same, but the flip must *not* coincide with a major merger.

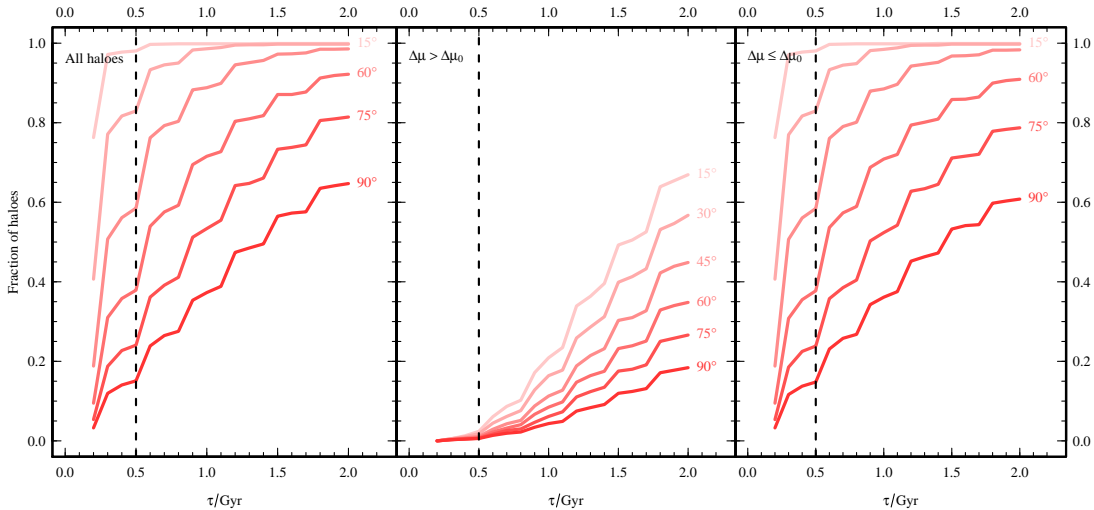


**Figure 7.** As Fig. 6, but for flips in the inner halo angular momentum.



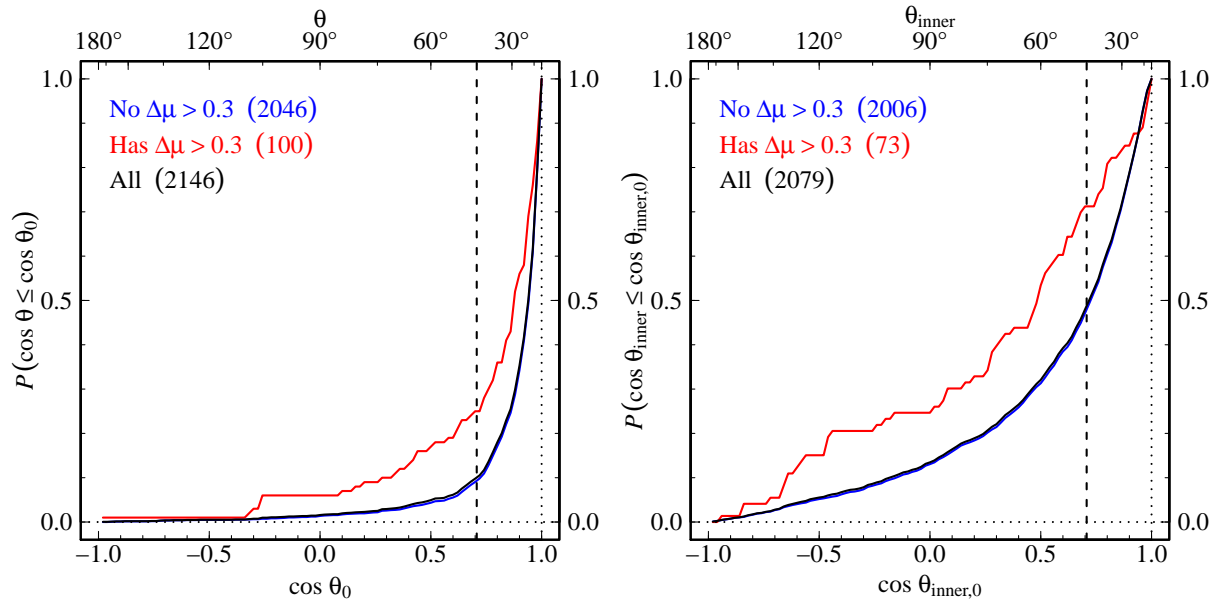


**Figure 8.** The cumulative fraction of MW final-mass haloes that have a spin flip (left: whole halo, right: inner halo) of at least  $\theta_0$  degrees at some point in their lifetime (black line). The other two lines correspond to the cases when the halo does (red) or does not (blue) have a major merger ( $\Delta\mu > 0.3$ ) during its lifetime. (The black line is almost coincident with the blue line.)

with a timescale of  $\tau = 0.5$  Gyr; 10.1 per cent of the haloes experience such a flip without it coinciding with a major merger. These percentages increase for longer timescales and smaller minimum angle change. Finally, we find that 9 per cent of the haloes that have not had *any* major merger after formation nevertheless have at least one spin flip of  $45^\circ$  or more.

The spin of the inner halo is subject to *larger* and *more frequent* changes in direction than the total halo spin, but like the total halo spin, inner spin flips also occur mainly without an accompanying major merger. Over half of the haloes have large inner spin flips at some point in their lifetimes without these coinciding with a major merger. For the haloes that do not experience any major mergers after formation, 47% experience a large inner halo spin flip. Large spin flips occur sufficiently frequently that they could have a significant impact on the evolution of the galactic baryonic material.

Our results suggest that a more complete understanding of the stability and resilience of galactic discs will require looking beyond mergers (major or minor) and internal instabilities and should include the role of spin flips which, as we have seen, can be quite common for the inner halo. The survivability of discs is not just determined by the halo potential. As has been shown in both models (e.g. Stewart et al. 2009; Hopkins et al. 2009a,b) and simulations (e.g. Okamoto et al. 2005; Scannapieco et al. 2009), the details of the baryonic physics – gas fraction, strength of supernova feedback, and other types of interaction between stars and gas – play a major role in whether a galactic disc lives or dies, or even can reform afterwards. Nevertheless, the behaviour of the underlying dark matter plays a critical role in galaxy formation. To understand how spin flips influence the evolution of discs will require full baryon physics simulations at high resolution. The handful of examples of simulations we have mentioned here already demonstrate that this process is both important and tractable.

## ACKNOWLEDGEMENTS

PEB thanks Peter Schneider & Christiano Porciani for helpful discussions, and acknowledges the support of the Deutsche Forschungsgemeinschaft under the project SCHN 342/7–1 in the framework of the Priority Programme SPP-1177, and the Initiative and Networking Fund of the Helmholtz Association, contract HA-101 (“Physics at the Terascale”). CSF acknowledges a Royal Society Wolfson Research Merit Award and an ERC Advanced Investigator grant. The simulations and analyses used in this paper were carried out as part of the programme of the Virgo Consortium on the Regatta supercomputer of the Computing Centre of the Max-Planck-Society in Garching, and the Cosmology Machine supercomputer at the Institute for Computational Cosmology, Durham. The Cosmology Machine is part of the DiRAC Facility jointly funded by STFC, the Large Facilities Capital Fund of BIS, and Durham University.

## REFERENCES

- Agustsson I., Brainerd T. G., 2010, *ApJ*, 709, 1321
- Allgood B., Flores R. A., Primack J. R., Kravtsov A. V., Wechsler R. H., Faltenbacher A., Bullock J. S., 2006, *MNRAS*, 367, 1781
- Avila-Reese V., Colín P., Gottlöber S., Firmani C., Maulbetsch C., 2005, *ApJ*, 634, 51
- Bailin J., Steinmetz M., 2005, *ApJ*, 627, 647
- Barnes J., Efstathiou G., 1987, *ApJ*, 319, 575
- Barnes J. E., 1988, *ApJ*, 331, 699
- , 1992, *ApJ*, 393, 484
- Barnes J. E., Hernquist L., 1996, *ApJ*, 471, 115
- Baugh C. M., 2006, *Reports on Progress in Physics*, 69, 3101
- Benson A. J., 2010, *Phys. Rep.*, 495, 33
- Bett P., Eke V., Frenk C. S., Jenkins A., Helly J., Navarro J., 2007, *MNRAS*, 376, 215

- Bett P., Eke V., Frenk C. S., Jenkins A., Okamoto T., 2010, *MNRAS*, 404, 1137
- Bett P. E., 2010, in American Institute of Physics Conference Series, Vol. 1240, American Institute of Physics Conference Series, V. P. Debattista & C. C. Popescu, ed., pp. 403–404
- Bett P. E., Frenk C. S., 2011, (in prep)
- Bournaud F., Jog C. J., Combes F., 2005, *A&A*, 437, 69
- Bower R. G., Benson A. J., Malbon R., Helly J. C., Frenk C. S., Baugh C. M., Cole S., Lacey C. G., 2006, *MNRAS*, 370, 645
- Boylan-Kolchin M., Springel V., White S. D. M., Jenkins A., Lemson G., 2009, *MNRAS*, 398, 1150
- Brunino R., Trujillo I., Pearce F. R., Thomas P. A., 2007, *MNRAS*, 375, 184
- Bryan G. L., Norman M. L., 1998, *ApJ*, 495, 80
- Bullock J. S., Dekel A., Kolatt T. S., Kravtsov A. V., Klypin A. A., Porciani C., Primack J. R., 2001, *ApJ*, 555, 240
- Catelan P., Theuns T., 1996a, *MNRAS*, 282, 436
- , 1996b, *MNRAS*, 282, 455
- Chen D. N., Jing Y. P., Yoshikawa K., 2003, *ApJ*, 597, 35
- Cole S., Lacey C., 1996, *MNRAS*, 281, 716
- Colless M. et al., 2001, *MNRAS*, 328, 1039
- Cox T. J., Dutta S. N., Di Matteo T., Hernquist L., Hopkins P. F., Robertson B., Springel V., 2006, *ApJ*, 650, 791
- Cox T. J., Jonsson P., Somerville R. S., Primack J. R., Dekel A., 2008, *MNRAS*, 384, 386
- Croft R. A. C., Di Matteo T., Springel V., Hernquist L., 2009, *MNRAS*, 400, 43
- Cuesta A. J., Betancort-Rijo J. E., Gottlöber S., Patiri S. G., Yepes G., Prada F., 2008, *MNRAS*, 385, 867
- Davis M., Efstathiou G., Frenk C. S., White S. D. M., 1985, *ApJ*, 292, 371
- De Lucia G., Blaizot J., 2007, *MNRAS*, 375, 2
- De Lucia G., Boylan-Kolchin M., Benson A. J., Fontanot F., Monaco P., 2010, *MNRAS*, 406, 1533
- Deason A. J. et al., 2011, *MNRAS*, 415, 2607
- Doroshkevich A. G., 1970a, *Astrophysics*, 6, 320
- , 1970b, *Astrofizika*, 6, 581
- Efstathiou G., Jones B. J. T., 1979, *MNRAS*, 186, 133
- Eke V. R., Cole S., Frenk C. S., 1996, *MNRAS*, 282, 263
- Fakhouri O., Ma C., 2008, *MNRAS*, 386, 577
- , 2009, *MNRAS*, 394, 1825
- Fall S. M., Efstathiou G., 1980, *MNRAS*, 193, 189
- Faltenbacher A., Allgood B., Gottlöber S., Yepes G., Hoffman Y., 2005, *MNRAS*, 362, 1099
- Freeman K. C., 2008, in IAU Symposium, Vol. 245, IAU Symposium, M. Bureau, E. Athanassoula, & B. Barbuy, ed., pp. 3–10
- Frenk C. S., White S. D. M., Davis M., Efstathiou G., 1988, *ApJ*, 327, 507
- Gao L., Navarro J. F., Cole S., Frenk C. S., White S. D. M., Springel V., Jenkins A., Neto A. F., 2008, *MNRAS*, 387, 536
- Genel S., Genzel R., Bouché N., Naab T., Sternberg A., 2009, *ApJ*, 701, 2002
- Giocoli C., Moreno J., Sheth R. K., Tormen G., 2007, *MNRAS*, 376, 977
- Gustafsson M., Fairbairn M., Sommer-Larsen J., 2006, *Phys. Rev. D*, 74, 123522
- Hahn O., Carollo C. M., Porciani C., Dekel A., 2007a, *MNRAS*, 381, 41
- Hahn O., Porciani C., Carollo C. M., Dekel A., 2007b, *MNRAS*, 375, 489
- Hahn O., Teyssier R., Carollo C. M., 2010, *MNRAS*, 405, 274
- Harker G., Cole S., Helly J., Frenk C., Jenkins A., 2006, *MNRAS*, 367, 1039
- Hayashi E., Navarro J. F., Springel V., 2007, *MNRAS*, 377, 50
- Helly J. C., Cole S., Frenk C. S., Baugh C. M., Benson A., Lacey C., 2003, *MNRAS*, 338, 903
- Hernquist L., 1992, *ApJ*, 400, 460
- , 1993, *ApJ*, 409, 548
- Hopkins P. F. et al., 2010, *ApJ*, 715, 202
- Hopkins P. F., Cox T. J., Younger J. D., Hernquist L., 2009a, *ApJ*, 691, 1168
- Hopkins P. F. et al., 2009b, *MNRAS*, 397, 802
- Hoyle F., 1951, in Problems of Cosmical Aerodynamics, Burgers J. M., van de Hulst H. C., eds., Central Air Documents Office, Dayton, OH, pp. 195–197
- Knebe A., Gill S. P. D., Gibson B. K., Lewis G. F., Ibata R. A., Dopita M. A., 2004, *ApJ*, 603, 7
- Knebe A., Power C., 2008, *ApJ*, 678, 621
- Kormendy J., Kennicutt, Jr. R. C., 2004, *ARA&A*, 42, 603
- Lacey C., Cole S., 1993, *MNRAS*, 262, 627
- Lemson G., the Virgo Consortium, 2006, ArXiv Astrophysics e-prints (astro-ph/0608019)
- Li Y., Mo H. J., Gao L., 2008, *MNRAS*, 389, 1419
- Libeskind N. I., Frenk C. S., Cole S., Helly J. C., Jenkins A., Navarro J. F., Power C., 2005, *MNRAS*, 363, 146
- Libeskind N. I., Frenk C. S., Cole S., Jenkins A., Helly J. C., 2009, *MNRAS*, 399, 550
- Libeskind N. I., Knebe A., Hoffman Y., Gottlöber S., Yepes G., Steinmetz M., 2011, *MNRAS*, 411, 1525
- Łokas E. L., Mamon G. A., 2001, *MNRAS*, 321, 155
- Lovell M. R., Eke V. R., Frenk C. S., Jenkins A., 2011, *MNRAS*, 413, 3013
- Macciò A. V., Dutton A. A., van den Bosch F. C., 2008, *MNRAS*, 391, 1940
- Macciò A. V., Dutton A. A., van den Bosch F. C., Moore B., Potter D., Stadel J., 2007, *MNRAS*, 378, 55
- Maller A. H., Katz N., Kereš D., Davé R., Weinberg D. H., 2006, *ApJ*, 647, 763
- Mo H. J., Mao S., White S. D. M., 1998, *MNRAS*, 295, 319
- Muñoz-Cuartas J. C., Macciò A. V., Gottlöber S., Dutton A. A., 2011, *MNRAS*, 411, 584
- Naab T., Burkert A., 2003, *ApJ*, 597, 893
- Navarro J. F., Frenk C. S., White S. D. M., 1996, *ApJ*, 462, 563
- , 1997, *ApJ*, 490, 493
- Neto A. F. et al., 2007, *MNRAS*, 381, 1450
- Okamoto T., Eke V. R., Frenk C. S., Jenkins A., 2005, *MNRAS*, 363, 1299
- Ostriker E. C., Binney J. J., 1989, *MNRAS*, 237, 785
- Parry O. H., Eke V. R., Frenk C. S., 2009, *MNRAS*, 396, 1972
- Paz D. J., Stasyszyn F., Padilla N. D., 2008, *MNRAS*, 389, 1127
- Peebles P. J. E., 1969, *ApJ*, 155, 393
- , 1971, *A&A*, 11, 377
- Percival W. J. et al., 2002, *MNRAS*, 337, 1068
- Porciani C., Dekel A., Hoffman Y., 2002, *MNRAS*, 332, 325
- Romano-Díaz E., Shlosman I., Heller C., Hoffman Y., 2009, *ApJ*, 702, 1250
- Scannapieco C., White S. D. M., Springel V., Tissera P. B., 2009, *MNRAS*, 396, 696
- Schäfer B. M., 2009, International Journal of Modern Physics D, 18, 173
- Shaw L. D., Weller J., Ostriker J. P., Bode P., 2006, *ApJ*, 646, 815
- Sheth R. K., Tormen G., 2004, *MNRAS*, 349, 1464

- Sinha M., Holley-Bockelmann K., 2011, *ApJ*, submitted (arXiv:1103.1675)
- Spergel D. N. et al., 2003, *ApJS*, 148, 175
- Springel V. et al., 2005, *Nature*, 435, 629
- Springel V., White S. D. M., Tormen G., Kauffmann G., 2001, *MNRAS*, 328, 726
- Stewart K. R., Bullock J. S., Wechsler R. H., Maller A. H., 2009, *ApJ*, 702, 307
- Stewart K. R., Bullock J. S., Wechsler R. H., Maller A. H., Zentner A. R., 2008, *ApJ*, 683, 597
- Sugerman B., Summers F. J., Kamionkowski M., 2000, *MNRAS*, 311, 762
- Toomre A., 1977, in *Evolution of Galaxies and Stellar Populations*, B. M. Tinsley & R. B. Larson, ed., pp. 401–416
- Toomre A., Toomre J., 1972, *ApJ*, 178, 623
- Tweed D., Devriendt J., Blaizot J., Colombi S., Slyz A., 2009, *A&A*, 506, 647
- van den Bosch F. C., Abel T., Croft R. A. C., Hernquist L., White S. D. M., 2002, *ApJ*, 576, 21
- van den Bosch F. C., Abel T., Hernquist L., 2003, *MNRAS*, 346, 177
- Warren M. S., Quinn P. J., Salmon J. K., Zurek W. H., 1992, *ApJ*, 399, 405
- Wechsler R. H., Bullock J. S., Primack J. R., Kravtsov A. V., Dekel A., 2002, *ApJ*, 568, 52
- White S. D. M., 1984, *ApJ*, 286, 38
- White S. D. M., Frenk C. S., 1991, *ApJ*, 379, 52
- White S. D. M., Rees M. J., 1978, *MNRAS*, 183, 341
- Zavala J., Okamoto T., Frenk C. S., 2008, *MNRAS*, 387, 364